Volume 46
Number 10
14 March 2017
Pages 3073-3412

Dalton Transactions

An international journal of inorganic chemistry

rsc.li/dalton

ISSN 0306-0012

COMMUNICATION
Douglas W. Stephan et al
N-Heterocyclic carbene stabilized parent sulfenyl, selenenyl,
and tellurenyl cations (XH⁺, X = S, Se, Te)

ROYAL SOCIETY
OF CHEMISTRY

This is an Accepted Manuscript, which has been through the Royal Society of Chemistry peer review process and has been accepted for publication.

Accepted Manuscripts are published online shortly after acceptance, before technical editing, formatting and proof reading. Using this free service, authors can make their results available to the community, in citable form, before we publish the edited article. We will replace this Accepted Manuscript with the edited and formatted Advance Article as soon as it is available.

You can find more information about Accepted Manuscripts in the Information for Authors.

Please note that technical editing may introduce minor changes to the text and/or graphics, which may alter content. The journal's standard Terms & Conditions and the Ethical guidelines still apply. In no event shall the Royal Society of Chemistry be held responsible for any errors or omissions in this Accepted Manuscript or any consequences arising from the use of any information it contains.

ARTICLE TYPE

www.rsc.org/xxxxxx | XXXXXXXX

Novel synthesis of NiMoP phosphide catalyst in a CH$_4$-CO$_2$ gas mixture

Zhichao Li,[a] Qingyou Liu,*[b] Yan Shi,[a] Zhiwei Yao,*[a] Wei Ding[a] and Yue Sun[a]

NiMo bimetallic phosphide was synthesized from corresponding oxidic precursor in a 1:1 CH$_4$:CO$_2$ gas mixture for the first time. The in-situ synthesized NiMoP phase in the feed for CH$_4$-CO$_2$ reforming can exhibit higher activity than the one prepared in H$_2$.

Transition metal phosphides are a new class of interstitial compounds receiving much attention in recent years due to their widespread applications in various fields, such as electronics, photonics, magnetism, catalysis and so on.[1-4] In particular, monometallic (e.g. MoP and Ni$_2$P) and bimetallic (e.g. NiMoP and CoMoP) phosphides have been identified as potential catalysts for many reactions such as hydrogenation and hydrotreating,[5,6] dry (CO$_2$) reforming of methane (DRM),[7,8] N$_2$H$_4$ decomposition[9,10] NO dissociation[11] and electrocatalytic reactions including hydrogen evolution, oxygen reduction and evolution reactions.[12-14]

Generally, phosphide catalysts are typically prepared by temperature programmed reduction (TPR) method, in which the reported reducing agents include H$_2$,[5] methane[15] and dimethyl ether.[16] Since the formation of phosphide from their corresponding oxidic precursors by H$_2$-TPR (Scheme 1)[17,18-24] is thermodynamically unfavorable, the forward reaction has to be aided by high temperature and low water vapor pressure. Thus, phosphides can only be obtained at a low heating rate (e.g. 1 °C min^{-1}) and a high H$_2$ flow speed (e.g. 300 ml min^{-1})[5] to purge the water off the solid surface. In addition, a high concentration of water produced during the reaction process can lead to serious hydrothermal sintering of phosphide particles.[25,26] In the case of the synthesis using methane and dimethyl ether as reducing agents, the resultant phosphide surface is usually contaminated by carbon deposition from the pyrolysis of CH$_4$, which can block in the pores and cover the active sites.[15,16] In this work, we developed a novel synthesis of NiMo bimetallic phosphide catalyst in a 1:1 CH$_4$:CO$_2$ gas mixture. Compared with the TPR method using H$_2$, methane and dimethyl ether as reducing agents, the reaction products included a large amount of CO and H$_2$ besides H$_2$O in this novel synthesis route, which can mitigate hydrothermal sintering of phosphide particles and avoid carbon deposition on the surface. Moreover, the in-situ synthesized NiMoP catalyst in the feed for DRM could exhibit higher activity than the one prepared in H$_2$.

$$zMO_x(s)+PO_y(s)+(zx+y)H_z(g) \xrightleftharpoons[very\ fast]{slow} M_zP(s)+(zx+y)H_zO(g)$$
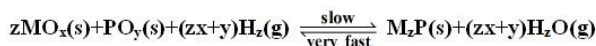
Scheme 1 A simplified equation for the preparation of phosphides by H$_2$-TPR method.

Fig. 1 shows the XRD patterns of the products from Ni$_x$Mo$_y$P$_1$ oxidic precursors with different Ni:Mo molar ratios in CH$_4$/CO$_2$ gas mixture. In the case of treating Ni$_x$Mo$_1$P$_1$ (x=0, 0.3, 0.6, 1) precursors, the XRD pattern of the product from Ni$_0$Mo$_1$P$_1$ showed the peaks of MoOPO$_4$ (main peaks at 2θ=25.2, 28.9, 38.7 and 41.3°, PDF 73-2333), indicating that Mo phosphide cannot be in-situ synthesized during DRM. When the Ni (x=0.3) was added into the precursor, the product was composed of MoOPO$_4$, MoO$_2$ (main peaks at 2θ=26.0, 36.9, 37.0 and 53.4°, PDF 78-1071) and Ni$_2$P$_2$O$_7$ (main peaks at 2θ=29.6 and 30.6°, PDF 49-1082). With the increase of Ni content from x=0.3 to x=0.6, the MoOPO$_4$ reflections disappeared, and some weak peaks due to MoP (2θ=32.0 and 43.0°, PDF 65-6487) and NiMoP (main peaks at 2θ=39.2, 43.2 and 47.3°, PDF 31-0873) were detected. With a further increase of Ni content to x=1, the phase composition of the product was predominant NiMoP with very minor Ni$_{12}$P$_5$ (main peaks at 2θ=38.4, 41.8, 47.0 and 48.9°, PDF 74-1381) and Mo$_3$P (main peaks at 2θ=38.0, 42.4, 45.8 and 47.3°, PDF 89-2587). As for Ni$_1$Mo$_y$P$_1$ (y=0, 0.3, 0.6, 1) precursors, they all were reduced to phosphide phases. Note that there was a clear main phase transformation (NiMoP→Ni$_x$Mo$_y$P[27]→Ni$_x$P) with decreasing Mo content from y=1 to y=0 in the oxidic precursors. The results indicated that the increase of Ni/Mo molar ratio in the oxidic precursors can promote the formation of phosphide phase and well crystalline NiMoP phase can be obtained with a stoichiometric ratio of 1:1:1 Ni:Mo:P. The XRD result was in good agreement with the result of H$_2$-TPR (Fig. 2) that the Ni$_1$Mo$_0$P$_1$ was more easily reduced than Ni$_0$Mo$_1$P$_1$ and the addition of Ni to precursor can facilitate precursor reduction.
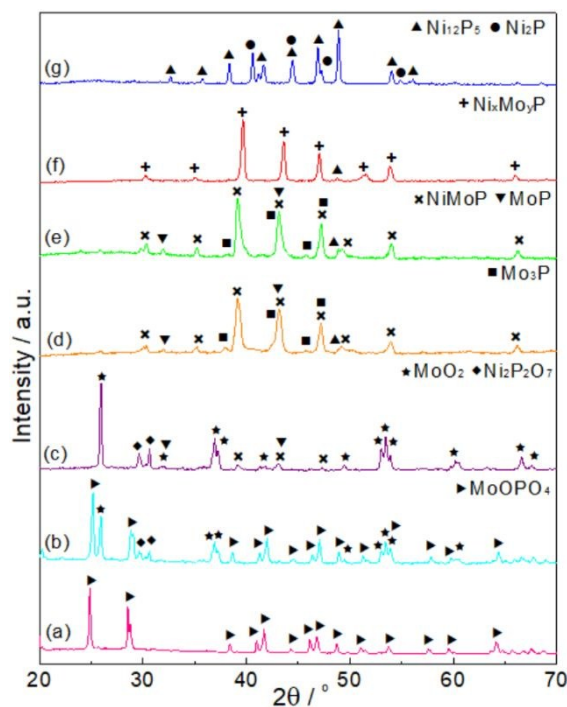

Fig. 1 XRD patterns of materials generated from the Ni$_x$Mo$_y$P$_1$ oxidic precursors with different Ni:Mo molar ratios in CH$_4$/CO$_2$ gas mixture at 900 °C for 5 h. (a) x=0, y=1, (b) x=0.3, y=1, (c) x=0.6, y=1, (d) x=1, y=1, (e) x=1, y=0.6, (f) x=1, y=0.3 and (g) x=1, y=0.

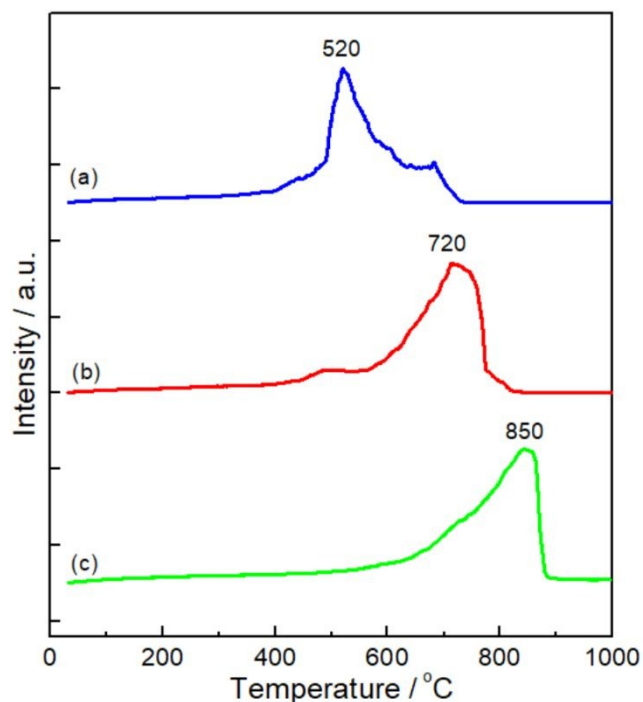Fig. 2 Profiles of H_2-TPR of (a) $Ni_1Mo_0P_1$, (b) $Ni_1Mo_1P_1$ and (c) $Ni_0Mo_1P_1$ precursors.

Whereafter, XPS analysis was used to further determine the surface composition of as-prepared NiMoP sample from $N_1Mo_1P_1$. Fig. 3 shows the XPS spectra of Ni 2p, Mo 3d and P 2p levels for the NiMoP sample. It can be seen that the surface region of the sample was composed of oxidized species and phosphorized species. The binding energies of oxidized Ni (856.0 eV), Mo (228.8 and 232.5 eV) and P (133.1 eV) were agreed with assignments by others to Ni^{2+}, Mo^{4+}/Mo^{6+} and P^{5+} species,[28,29] respectively. The binding energies of the peaks at 853.3, 227.9 and 129.8 eV were attributed to $Ni^{\alpha+}$, $Mo^{\delta+}$ and $P^{\sigma-}$ in phosphide,[23,26] respectively. The detection of these oxidized species should be attributed to surface oxidation of phosphide in the passivation process.[29]
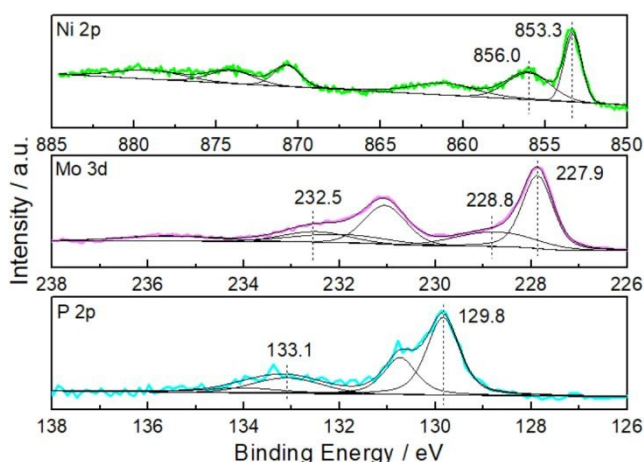

Fig. 3 XPS spectra of Ni 2p, Mo 3d and P 2p regions of NiMoP sample prepared from $Ni_1Mo_1P_1$ oxidic precursor.
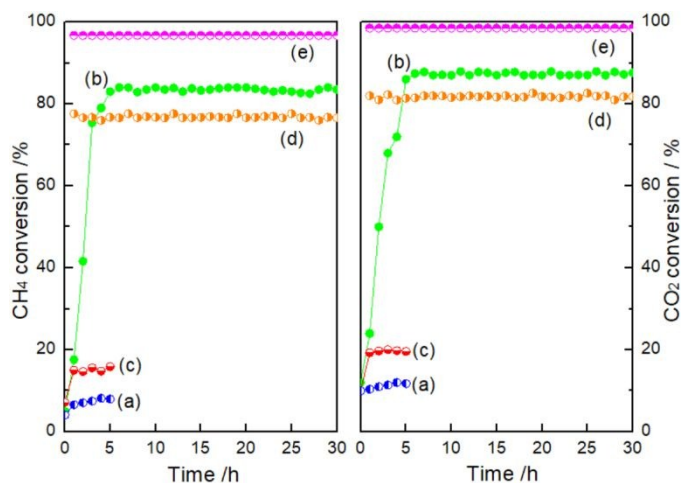

Fig. 4 SEM (a) and TEM (b) images of NiMoP sample prepared from $Ni_1Mo_1P_1$ oxidic precursor in CH_4/CO_2 gas mixture.

Fig. 5 Catalytic activity of the (a) $Ni_0Mo_1P_1$, (b) $Ni_1Mo_1P_1$, (c) $Ni_1Mo_0P_1$ precursors, (d) H_2-NiMoP in DRM and (e) estimated values of conversions at the reaction equilibrium. Reaction conditions: $CH_4:CO_2=1:1$, WHSV=9000 cm^3 g^{-1} h^{-1}, reaction pressure= 1 atm, reaction temperature=900 ^oC.

Additionally, the morphology of as-prepared NiMoP sample (hereafter denoted as CH_4/CO_2-NiMoP) from $N_1Mo_1P_1$ was characterized by SEM and TEM. As shown in SEM image (Fig. 4a), the product consisted of aggregates of irregularly rod-shaped particles. The SEM result was in good agreement with the observation of TEM image (Fig. 4b). However, the NiMoP sample (hereafter denoted as H_2-NiMoP) obtained by H_2-TPR consisted of large aggregates of particles (Fig. S1), indicating that serious hydrothermal sintering occurred in this synthesis process.[30] Therefore, the surface area of CH_4/CO_2-NiMoP (8.1 m^2 g^{-1}) was higher than that of H_2-NiMoP (4.2 m^2 g^{-1}). In addition, CHN analysis result showed no carbon in the CH_4/CO_2-NiMoP sample, indicating that no carbon deposition formed in the synthesis process.
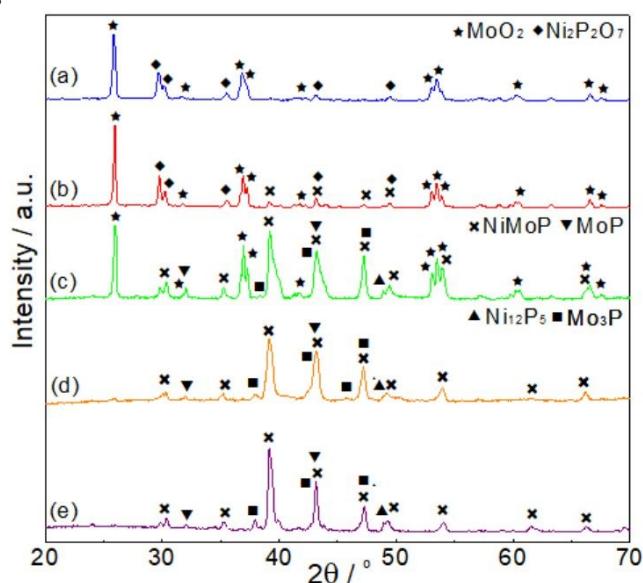

Fig. 6 XRD patterns of the products obtained from $Ni_1Mo_1P_1$ precursor with different time in CH_4/CO_2 at 900 ºC. (a) 0 h, (b) 1 h, (c) 3 h, (d) 5 h and (e) 30 h.

The catalytic activity of the $Ni_0Mo_1P_1$, $Ni_1Mo_1P_1$ and $Ni_1Mo_0P_1$ precursors in DRM was investigated at 900 ºC (Fig. 5). Among the three samples, the $Ni_0Mo_1P_1$ precursor exhibited the poorest activity with CH_4 and CO_2 conversions of ca. 7 and 10%, respectively within a period of 5 h. This was because the $Ni_0Mo_1P_1$ precursor cannot be reduced to MoP in CH_4/CO_2 gas mixture (see Fig. 1) and the $MoOPO_4$ product was almost not active for DRM. In the case of the $Ni_1Mo_1P_1$ and $Ni_1Mo_0P_1$ precursors, there was a rapid increase in CH_4 and CO_2 conversions in the initial period, which should be attributed to the in-situ formation of NiMoP from $Ni_1Mo_1P_1$ and Ni_xP from $Ni_1Mo_0P_1$, as suggested by XRD result (see Fig. 1). Note that the NiMoP (X_{CH4}=~83% and X_{CO2}=~87%) showed much higher CH_4 and CO_2 conversions than Ni_xP (X_{CH4}=~15% and X_{CO2}=~19%) when the reaction proceeded to reach its steady state. In addition, the high activity and selectivity (see Fig. S2) can be maintained over the catalyst for the duration of the experiment of 30 h and there was almost no change on the catalyst structure during the reaction from 5 to 30 h, as proved later by XRD. For the sake of

comparison, the DRM performance of NiMoP catalyst prepared in H_2 was also investigated under similar reaction conditions (see Figs. 5 and S2). It can be seen that the conversions over both CH_4/CO_2-NiMoP and H_2-NiMoP were far away from the values (X_{CH4}=~96% and X_{CO2}=~98%) at the reaction equilibrium.[31] And the conversions over CH_4/CO_2-NiMoP were slightly higher (about 6%) than those over H_2-NiMoP under a WHSV=9000 cm^3 g^{-1} h^{-1}. When the WHSV was increased to 24000 cm^3 g^{-1} h^{-1}, the values of X_{CH4} and X_{CO2} for CH_4/CO_2-NiMoP were above 10% higher than those for H_2-NiMoP (Fig. S3). These results should be mainly attributed to its higher surface area and better particle dispersion (see Figs. 4 and S1).

Finally, in order to investigate the formation process of the NiMoP in CH_4/CO_2 gas mixture, some intermediate samples were characterized. Fig. 6 shows the XRD patterns of the products obtained from $Ni_1Mo_1P_1$ precursor with different time in CH_4/CO_2 at 900 ºC. At 0 h, the precursor was transformed into a mixture phase of MoO_2 and $Ni_2P_2O_7$. This mixture should also include amorphous PO_x.[25] When the time increased to 1 h, a small amount of desired product NiMoP had appeared. With further increasing time, the intensity of the MoO_2 and $Ni_2P_2O_7$ peaks gradually decreased, and the $Ni_1Mo_1P_1$ precursor had been basically transformed into a single NiMoP phase at 5 h except a small quantity of Mo_3P and $Ni_{12}P_5$ phases.
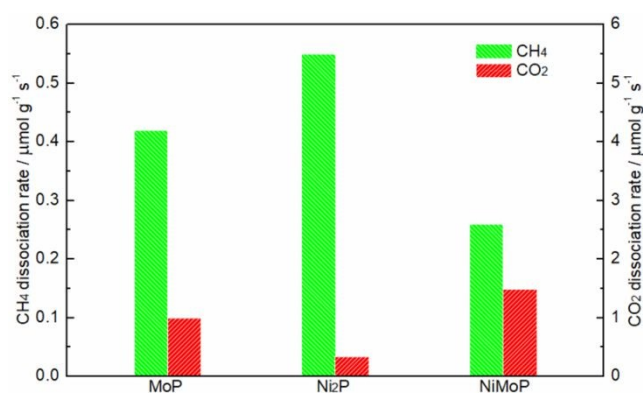

Fig. 7 Dissociation rates of CH_4 and CO_2 over MoP, Ni_2P and NiMoP catalylsts. Reaction conditions: CH_4:Ar=1:50, CO_2:Ar=1:50, WHSV=30000 cm^3 g^{-1} h^{-1}, reaction time=10 min, reaction temperature= 900 ºC.

It had been confirmed from XRD that $Ni_2P_2O_7$ can be reduced easily to Ni_xP in CH_4/CO_2 (see Figs. 1 and 2). And the CH_4 and CO_2 dissociation studies (Fig. 7) indicated that the Ni_2P exhibited relatively high activity for CH_4 dissociation but relatively low activity for CO_2 dissociation. Therefore, it was reasonable to deduce that once the Ni_xP was formed, the Mo species might be reduced to Mo_xP by H_2 from CH_4 dissociation over Ni_xP. It was also found from Fig. S4 that the Ni phosphide can directly react with the Mo phosphide to form Ni_xMo_yP.[27] Thus, the formation process of NiMoP from $Ni_1Mo_1P_1$ precursor was proposed as follows: (i) the Ni_xP was formed in CH_4/CO_2; (ii) the Mo_xP was formed in Ni_xP-catalyzed CH_4 dissociation; (iii) the Ni_xP reacted with

Mo_xP to produce NiMoP. Note that the reaction products included a large amount of CO and H_2 besides H_2O, which can mitigate the hydrothermal sintering of phosphide particles and avoid carbon deposition on the surface.

Conclusions

In summary, we developed a novel in-situ approach to produce NiMoP catalyst in CH_4-CO_2 for the DRM. In this method, first the Ni_xP was formed and then the Mo_xP was formed in Ni_xP-catalyzed CH_4 dissociation. Finally, the Ni_xP reacted with Mo_xP to produce NiMoP. Compared with traditional H_2-TPR method, the reaction products included a large amount of CO and H_2 besides H_2O in this novel synthesis route, which can mitigate hydrothermal sintering of phosphide particles. The in-situ synthesized NiMoP in CH_4-CO_2 showed higher DRM activity than the NiMoP catalyst prepared in H_2, which should be mainly attributed to its higher surface area and better particle dispersion.

Acknowledgements

Notes and references

aCollege of Chemistry, Chemical Engineering and Environmental Engineering, Liaoning Shihua University, Fushun, 113001, P.R. China
E-mail: mezhiwei@163.com

bKey Laboratory of High-temperature and High-pressure Study of the Earth's Interior, Institute of Geochemistry, Chinese Academy of Sciences, Guiyang, 550081, P.R. China
E-mail: liuqingyou@vip.gyig.ac.cn

1 A.-M. Alexander and J.S.J. Hargreaves, *Chem. Soc. Rev.*, 2010, **39**, 4388-4401.
2 E.J. Popczun, J.R. McKone, C.G. Read, A.J. Biacchi, A.M. Wiltrout, N.S. Lewis and R.E. Schaak, *J. Am. Chem. Soc.*, 2013, **135**, 9267-9270.
3 K.Y. Yoon, Y. Jang, J. Park, Y. Hwang, B. Koo, J.-G. Park and T. Hyeon, *J. Solid State Chem.*, 2008, **181**, 1609-1613.
4 X.C. Jiang, Q.H. Xiong, S. Nam, F. Qian, Y. Li and C.M. Lieber, *Nano Lett.*, 2007, **7**, 3214-3218.
5 C. Stinner, R. Prins and Th. Weber, *J. Catal.*, 2001, **202**, 187-194.
6 R. Wang and K.J. Smith, *Appl. Catal. A*, 2009, **361**, 18-25.
7 Z. Yao, F. Luan, Y Sun, B. Jiang and J. Song, *Catal. Sci. Technol.*, 2016, **6**, 7996-8004.
8 Y. Cui, Q. Liu, Z. Yao, B. Dou, Y. Shi and Y. Sun, *Int. J. Hydrogen Energy*, 2019, **44**, 11441-11447.
9 M. Zheng, Y. Shu, J. Sun and T. Zhang, *Catal. Lett.*, 2008, **121**, 90-96.
10 R. Cheng, Y. Shu, M. Zheng, L. Li, J. Sun, X. Wang and T. Zhang, *J. Catal.*, 2007, **249**, 397-400.
11 Z.W. Yao, H. Dong and Y. Shang, *J. Alloys Compd*, 2009, **474**, L10-13.
12 Y. Lv and X. Wang, *Catal. Sci. Technol.*, 2017, **7**, 3676-3691.
13 E.J. Popczun, C.G. Read, C.W. Roske, N.S. Lewis and R. E. Schaak, *Angew. Chem.*, 2014, **126**, 5531-5534.
14 L. Feng, H. Vrubel, M. Bensimon and X. Hu, *Phys. Chem. Chem. Phys.*, 2014, **16**, 5917-5921.
15 S. Burns, J.S.J. Hargreaves and S.M. Hunter, *Catal. Commun.*, 2007, **8**, 931-935.
16 Z. Yao, M. Li, X. Wang, X. Qiao, J. Zhu, Y. Zhao, G. Wang, J. Yin and H. Wang, *Dalton T.*, 2015, **44**, 5503-5509.
17 A. Wang, M. Qin, J. Guan, L. Wang, H. Guo, X. Li, Y. Wang and R. Prins, *Angew. Chem.*, 2008, **120**, 6141-6143.
18 V. Zuzaniuk and R. Prins, *J. Catal.*, 2003, **219**, 85-96.
19 R. Wang and K.J. Smith, *Appl. Catal. A*, 2009, **361**, 18-25.
20 B. Guichard, M. Roy-Auberger, E. Devers, C. Legensb and P. Raybaudc, *Catal. Today*, 2008, **130**, 97-108.
21 S. Izhar and M. Nagai, *Catal. Today*, 2009, **126**, 172-176.
22 M. Nagai, T. Fukiage and S. Kurata, *Catal. Today*, 2005, **106**, 201-205.
23 J. Chen, Y. Yang, H. Shi, M. Li, Y. Chu, Z. Pan and X. Yu, *Fuel*, 2014, **129**, 1-10.
24 K Li, R Wang, J Chen, *Energy Fuels*, 2011, **25**, 854-863.
25 Z. Yao, J. Tong, X. Qiao, J. Jiang, Y. Zhao, D. Liu, Y. Zhang and H. Wang, *Dalton Trans.*, 2015, **44**, 19383-19391.
26 Z. Yao, G. Wang, Y. Shi, Y. Zhao, J. Jiang, Y. Zhang and H. Wang, *Dalton Trans.*, 2015, **44**, 14122-14129.
27 D. Ma, T.C. Xiao, S.H. Xie, W.Z. Zhou, S.L.Gonzalez-Cortes and M.L.H. Green, *Chem. Mater.*, 2004, **16**, 2697-2699.
28 P. Xiao, M.A. Sk and L. Thia, X.M. Ge, J.Y. Wang, K.H. Lim, R.J. Lim and X.Wang, *Energy Environ. Sci.*, 2014, **7**, 2624-2629.
29 A.W. Burns, A.F. Gaudette and M.E. Bussell, *J. Catal.*, 2008, **260**, 262-269.
30 Q. Guan, X. Cheng, R. Li and W. Li, *J. Catal.*, 2013, **299**,1-9.
31 J. Li, C. Chen, D. Wang, W. Yao and S. Zhang, *Chem. Eng. Oil Gas*, 2015, **44**, 60-64.